BATCH: jp9d48 USER: jld69 DIV: @xyv04/data1/CLS_pj/GRP_jp/JOB_i38/DIV_jp0102567 DATE: August 31, 2001

Molecular Dynamics Simulation of Microstructure and Molecular Mobilities in Swollen Nafion Membranes

Aleksey Vishnyakov and Alexander V. Neimark*

Center for Modeling and Characterization of Nanoporous MaterialsTRI/Princeton, 601 Prospect Avenue, Princeton, New Jersey 08542

Received: January 22, 2001; In Final Form: June 26, 2001

The microphase segregation in the Nafion (DuPont trademark) perfluorinated membrane at different water contents was studied using molecular dynamics simulations. As the degree of solvation increased, we observed the formation of water clusters containing up to ca. 100 water molecules. In contrast to the conventional network models, the water clusters do not form a continuous hydrophilic subphase. The cluster size distribution is rather wide and evolves in time due to formation and break-up of temporary bridges between the clusters. This dynamic behavior of the cluster system allows for the macroscopic transfer of water and counterion. The calculated diffusion coefficients of water were found to be on the same order as the experimental ones.

1. Introduction

A better understanding of the structure and transport properties of solvated Nafion membranes is of practical interest for water electrolysis, chlor-alkali technologies, electroorganic synthesis, catalysis, separations, sensors, electrode coating, and, in particular, for hydrogen and methanol fuel cells, which are seen today as the most promising energy suppliers for vehicles.[1−4] Due to sufficient water vapor and air permeability,[5] outstanding chemical, thermal and mechanical stability, small heat accumulation, and reduced weight, Nafion type perfluorinated polymers open new prospects for producing permselective membranes for packaging and protective clothing.

A Nafion macromolecule consists of a hydrophobic perfluorocarbon backbone with side chains terminated by the hydrophilic SO_3^- groups with counterions. The chemical formula of Nafion is shown as follows:

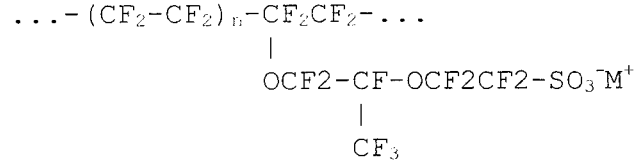

When exposed to water or some other hydrophilic solvents, a Nafion membrane swells and undergoes a microphase segregation. Solvent molecules and counterions form an aqueous, or hydrophilic, subphase around the hydrophilic side chains. The perfluorocarbon backbone constitutes an organic, or hydrophobic, subphase.

Significant experimental and theoretical efforts were put into the characterization of the microstructure of dry and swollen Nafion membranes.[6] Although the fact of microphase segregation and its influence on the thermodynamic and transport properties of Nafion membranes is well-established,[4] the morphology of the subphases in swollen Nafion membranes remains undetermined. Since swollen membranes exhibit high conductivity and water permeability, it is generally assumed that the hydrophilic phase is continuous. The conventional model of microphase segregation in Nafion membranes was put forward by Gierke et al. in the early 80's.[7,8] Based on the data of wide- and small- angle X-ray scattering (SAXS), Gierke et al. [7,8] have assumed that water and the counterions form nearly spherical clusters of 3−5 nm in diameter, which are randomly distributed in the hydrophobic matrix. Water diffuses between the clusters through narrow (ca. 1 nm in diameter) cylindrical channels. As the water content increases, the clusters grow in size, and the cluster connectivity becomes more pronounced. The model of Gierke at al. was modified by Mauritz and Rogers [9] and recently by Eikerling et al.[10] However, there are no direct data on the shape and size of hydrophilic clusters.

According to the neutron diffraction studies of Pineri et al.,[11] the size of the water clusters in Nafion under saturation conditions amounts to a few tens of nanometers, which is much larger than the estimate made by Gierke et al.[7,8] Falk [12] concluded from infrared spectroscopy studies that the water aggregates are much smaller than estimated by Gierke et al.[7,8] or they have a nonspherical shape. Plate and Shibaev [13] found the behavior of hydrated Nafion membranes to be similar to that of brushlike polymers and suggested a multilayer structure with lamellae water aggregates. The lamellae structure was supported by the results of neutron diffraction and Moessbauer spectroscopy experiments.[14] Tovbin[15] interpreted SAXS data from reference 16, assuming that the water aggregates have either a slitlike or a cylindrical shape. The estimated pore widths were ca. 40% lower than those of Gierke and Hsu.[7] Meresi et al.[17] studied dry and water swollen acid form membranes by Xenon-129 NMR. They found that in a dry membrane, the estimated size of hydrophilic domains was about 3.8 nm, with an overall periodicity of 10 nm. In a swollen membrane, the size of hydrophilic domains increased to 6.5 nm, while the overall periodicity remained the same. No particular conclusions regarding the possible shape and connectivity of hydrophilic domains were made. Recently, James et al. and Eliott et al.[18,19] investigated Nafion membranes in different degrees of hydration by two complementary techniques: atomic force microscopy (AFM) and SAXS combined with the maximum entropy reconstruction. The AFM images were found to support a cluster

* To whom correspondence should be addressed. E-mail aneimark@triprinceton.org.

10.1021/jp0102567 CCC: $20.00
Published on Web 00/00/0000 PAGE EST: 8.5

model of ionic aggregation, which has a hierarchical scale of structure: individual spheroidal ionic clusters of 3−5 nm in diameter are agglomerated into larger scale aggregates. Gebel[20] also studied the evolution of Nafion microstructure from dry materials to highly swollen membranes by means of SAXS. At the water content of ca. 50% volume, a modification in the swelling process was observed. Such behavior was attributed to an inversion of a reverse micellar structure to a connected network of rodlike particles. Orfino and Holdcroft,[21] in their recent SAXS study, questioned the existence of channels between the individual hydrophilic clusters. They estimated distances of separation between the surfaces of two adjacent hydrated clusters in air-dried and swollen Nafion membranes as 0.3 and 0.88 nm, respectively, which does not contradict with the existence of channels between the neighboring clusters. Gong et al.[22] studied self-diffusion water, ethanol, and decafluoropentane in Nafion using pulse gradient proton NMR. Analyzing the concentration dependence of the self-diffusion coefficients, the authors concluded that ethanol plasticizes Nafion more readily, producing larger domains than does water. Unlike water and methanol, decafluoropentane is supposed to interact strongly with the hydrophobic skeleton and, therefore, diffuse through the hydrophobic subphase. The diffusion constant of decafluoropentane turned out to depend strongly on the time interval during which the molecular mobility was measured. The authors concluded that the hydrophobic subphase contains large ordered regions where the perfluorocarbon backbone is crystalline. Diffusion through these regions is very slow or practically absent, thus severely restricting the decafluoropentane mobility.

The examples described above show that the structure and mechanisms of diffusion in perfluorinated membranes are poorly understood due to the lack of reliable interpretation of experimental data. In this situation, virtual experiments by means of molecular simulations come to the forefront. Molecular simulations have also been employed for studying Nafion. Ab initio energy optimization on the Nafion side chain was performed by Paddisson and Zawodzinski.[23] Vasyutkin and Tovbin[24] estimated the heat of water sorption in Nafion and energy barrier of H^+ and Li^+ ion exchange between neighboring SO_3^- group in a hydrated membrane using semiempirical molecular orbital calculations. Din and Michaelides[25] reported molecular dynamics (MD) simulations of diffusion of water and protons in Nafion. The polyelectrolite was modeled as a network of cylindrical pores of 0.936 and 1.224 nm in diameter with negatively charged walls. Similar simulations of water diffusion in slit-shaped pores of Li^+ Nafion were performed by Dyakov and Tovbin.[26] It should be noted that the authors of references 24−26 assumed a particular shape of hydrophilic aggregates in advance. Other solid polyelectrolytes have also been modeled. Ennari et al.[27] recently reported atomistic level molecular modeling of poly(ethylene oxide)sulfonic acid in water. The conductivity of the system, as well as diffusion coefficients for water, proton, and sulfonic anion were found to be in reasonable agreement with experiments. Ljubartsev and Laaksonen[28] studied solvation of DNA in the presence of different counterions (Li^+, Na^+, Cs^+). They found qualitative differences between the behaviors of counterions. The observed differences in ion binding to DNA may explain different conformational behaviors of DNA. The calculated self-diffusion coefficients were found to be in good agreement with those obtained from NMR studies. Ion clustering was observed in systems of lithium iodide dissolved in poly(ethylene) oxide by Muller-Plathe and van Gunsteren.[29] In our preceding work,[30,31] we considered solvation of Nafion oligomers in water, methanol, and a water−methanol mixture using static energy optimization and MD simulation. The attention was focused on the skeleton and side chain conformations, flexibility, and the molecular structure of the solvation shells around SO_3^- groups. In this paper, we report MD simulations of the microphase segregation in hydrated Nafion membranes at different water contents. The simulations were based on an empirical forcefield parametrized to fit selected experimental characteristics of smaller compounds containing the same molecular fragments as Nafion. This approach provides valuable information on the structure and diffusion in a swollen membrane supported by reasonable agreement between the simulation results and the experimental data on thermodynamic properties and water mobility. At the same time, apparent drawbacks of MD simulations should be noted. First, the size of the simulation cell and the timesacale of the detailed simulations are very limited and may notably affect the results. Second, the forcefield does not allow for thorough investigation of the structure of the hydrophobic subphase. In particular, it is not possible to determine whether crystalline domains[22] are present or not. We have found that water clusters do not form a continuous hydrophilic subphase. The cluster size distribution is rather wide and evolves in time due to the formation and break-up of temporary bridges between the clusters. This dynamic behavior of the cluster system allows for the macroscopic transfer of water and counterions. The calculated diffusion coefficients of water were found to be on the same order as the experimental ones.

2. Systems

All molecular simulations were performed at $T = 298$ K and $P = 1$ atm. Nafion polymer was represented by fifteen ten-unit oligomers with the equivalent weight 1164 (in the acid form), as described in the previous paper.[30] K^+ was considered as the counterion. That is, the simulation cell contained 150 SO_3^- groups and, correspondingly, 150 K^+ ions. The water content was varied. According to reference 32, the water content at saturation for Nafion 1200 in the K^+ form is 11.6−12.5 wt %. These data is close to that of Nandan et al.,[33] but differ considerably from the maximum water uptake reported by Gierke and Hsu,[7] who reported 8.7 wt % water content at saturation for the K^+ form of Nafion 1200.

We performed simulations at three different water contents: system (I) 5.0 wt %, which presumably corresponds to "intrinsic" water sorbed in Nafion; system (II) 12.5 wt %, which is assumed as the water content under saturation conditions; and system (III) 17.0 wt %, an unphysically high water content, which cannot be obtained in experiment. The content of 17 wt % corresponds to 1304 water molecules in the simulation box. For each system, the average density, the diffusion coefficients of water and K^+ ions, and the radial distribution functions were calculated.

3. Model and Forcefield

The model employed stems from the forcefield developed for the simulation of the solvation of Nafion oligomers.[30] However, studies of microphase segregation require computationally extensive simulations of larger systems. To expedite the simulations, we have simplified the forcefield[30] by using a united-atom presentation of CF_2 and CF_3 groups. In doing so, CF_2 and CF_3 groups are modeled as single Lennard−Jones (LJ) particles. For the perfluorohydrocarbon skeleton, we employed the model of Cui et al.[34] This model is based on the quantum density functional theory modeling of lower perfluoroalkanes

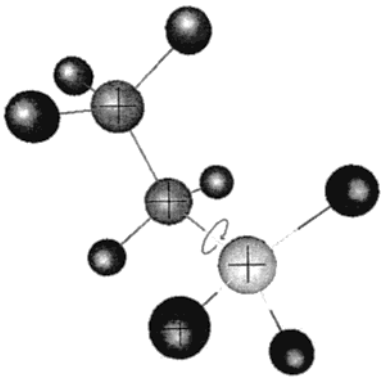

Figure 1. Fitting the torsion potential. The SO_3^- group is being rotated around the the C−S axis by 5−10 degree steps. At each step the potential energy is minimized with the O−S−C−C dihedral angle being fixed (the atoms which form the fixed dihedral are marked with black crosses).

TABLE 1: Sample Compounds, Torsion Potentials Fitted, and Corresponding Dihedrals of the Side Chain

sample compound	central dihedral	corresponding dihedrals of the side chain
SO_3-CF_2−CF_2	O−S−C−C	O5(O3,O4)-S−C5−C4
SO_3-CF_2-CF_2-O−CF_3	S−C−C−O	S−C5−C4−O2
CF_3-CF_2-O−CF_3	C−C−O−C	C2−O2−C4−C5
		C3−C2−O2−C4
		C1−C2−O2−C4
		C0−C1−O1−C2
CF_3-O-CF_2-CF_2-O−CF_3	O−C−C−O	O1−C1−C2−O2
CF_3-O-CF_2-CF_2−CF_3	O−C−C−C	O1−C1−C2−C3

up to perfluorooctane [35] and describes well the liquid properties and conditions of vapor−liquid equilibrium for perfluoroalkanes.[34]

Due to the lack of published data, it was difficult to find a suitable torsion potential for the united atom model of the side chain. We performed classical energy minimization on smaller compounds, which include the same dihedral angles as the Nafion side chain, using the all-atom forcefield developed for the previous simulations of the Nafion olygomers solvation in water and methanol.[30] The compounds chosen for this purpose are listed in Table 1. Each of the compounds has the center dihedral equivalent to one of the dihedrals of the side chain. The following optimization procedure was applied; the molecules were twisted around the central bond by steps of 5−10° each (depending on the symmetry, see Figure 1). At each step the potential energy minimization with a fixed central dihedral was performed using both the original all-atom forcefield and the simplified united-atom forcefield. Then, the torsion potential of the united-atom forcefield was fitted to match the potential energy obtained with the all-atom forcefield. The torsion potentials obtained by this procedure are given in Figure 2. The potentials were implemented into the Cerius^2 OFF module using the standard functions of the Cerius^2 forcefield editor. In this form, the potentials were assigned to the corresponding dihedral angles of the side chain (see Table 1).

The rigid three-center SPC/E model of Berendsen et al.[36] was used for the water molecule. Despite being relatively simple, the SPC/E model is capable of reproducing quite accurately the transport properties of pure liquid water. The K^+ ion was modeled as a charged Lennard−Jones atom according to reference 37.

4. Simulation Details

We performed molecular dynamics simulations of the hydrated Nafion membrane on a dual SGI Octane 300 workstation using the Cerius^2 OFF software package. The code was parallelized to use both processors of the workstation. We implemented the all-atom forcefield in the Cerius^2 OFF using the MSI forcefield editor. The torsion potentials obtained were fitted by standard functions implemented in the Cerius^2 OFF.

MD simulations of hydrated Nafion membranes were carried out in the NPT ensemble. In the NPT ensemble, the amount of each component in the simulation cell is fixed. The volume of the system is allowed to fluctuate to satisfy a given pressure, P. In so doing, the density of the system may deviate considerably from the experimental value. Equilibration is a common problem in molecular simulations of polymers, which makes the choice of initial configuration an important problem. We have attempted to obtain the initial configuration for the system II (12.5 wt % of water) by running the MSI Cerius^2 Amorphous Builder with the target density of 1.76 g/cm^3, which is close to the experimental density at these conditions. However, this approach was not successful. In the 1 ns simulation run started from this configuration, the equilibrium was not reached, which was indicated by a very slow water diffusion (we obtained $D_{H2O} = 1.3 \times 10^{-9}$cm^2/c, which is two orders lower than the experimental estimate of 1.2×10^{-7} cm^2/s) and an unreasonably high torsion potential energy.

To achieve the equilibration faster, we started from a very low-density configuration ($\rho = 0.02$ g/cm^3). The initial configurations were obtained using the MSI Cerius^2 Amorphous Builder. In the initial configuration, the simulation cell was cubic. In the process of NPT simulations, the edges of the cell, as well as the angles between the edges, were allowed to fluctuate independently, i.e., the cell had a triclinic shape. The maximum ratio between the length of the longest and the shortest edges of the cell was 1.06; the minimum angle between two edges was 86.7°. Within ca. 200 ps, the system was shrunk in the NPT simulation at $P = 10$ MPa to the density of 1.5 g/cm^3. The shape of the simulation cell was maintained as cubic during the shrinking. Then, the system was equilibrated at 1 atm within 400 ps until the density and potential energy of the system became stable. After that, statistics were collected for each trajectory over ca. 1 ns.

The equations of motion were integrated by the Verlet scheme,[38] with the time step of 1 fs. All covalent bonds were maintained rigid. Each 1 ps, the current configuration was saved for analyses. The temperature was maintained using the Nose−Hoover thermostat, with the cell mass prefactor of one and relaxation time of 0.3 ps.

In MD simulations of such complex systems, the key question is whether the equilibrium is reached. The profiles of equilibrium properties of the systems, such as the density and different contributions to the potential energy, did not show any notable trends within the trajectories over which the averaging was made. Thus, we assumed that our systems underwent transformations through a sequence of equilibrium states, either stable or metastable. However, we cannot estimate how representative the constructed trajectories are. In MD simulations of solutions with complex molecules, there is always a danger that the simulation trajectory covers only a narrow region of metastable states and, therefore, may be unrealistic. This problem is partly discussed below.

5. Results and Discussion

5.1 Densities. The average linear dimension of the simulation cell was 56.6, 57.3, and 59.4 Å at the water content of 5.0, 12.5, and 17 wt %, respectively. Table 2 shows the resulting densities and transport characteristics of all three systems.

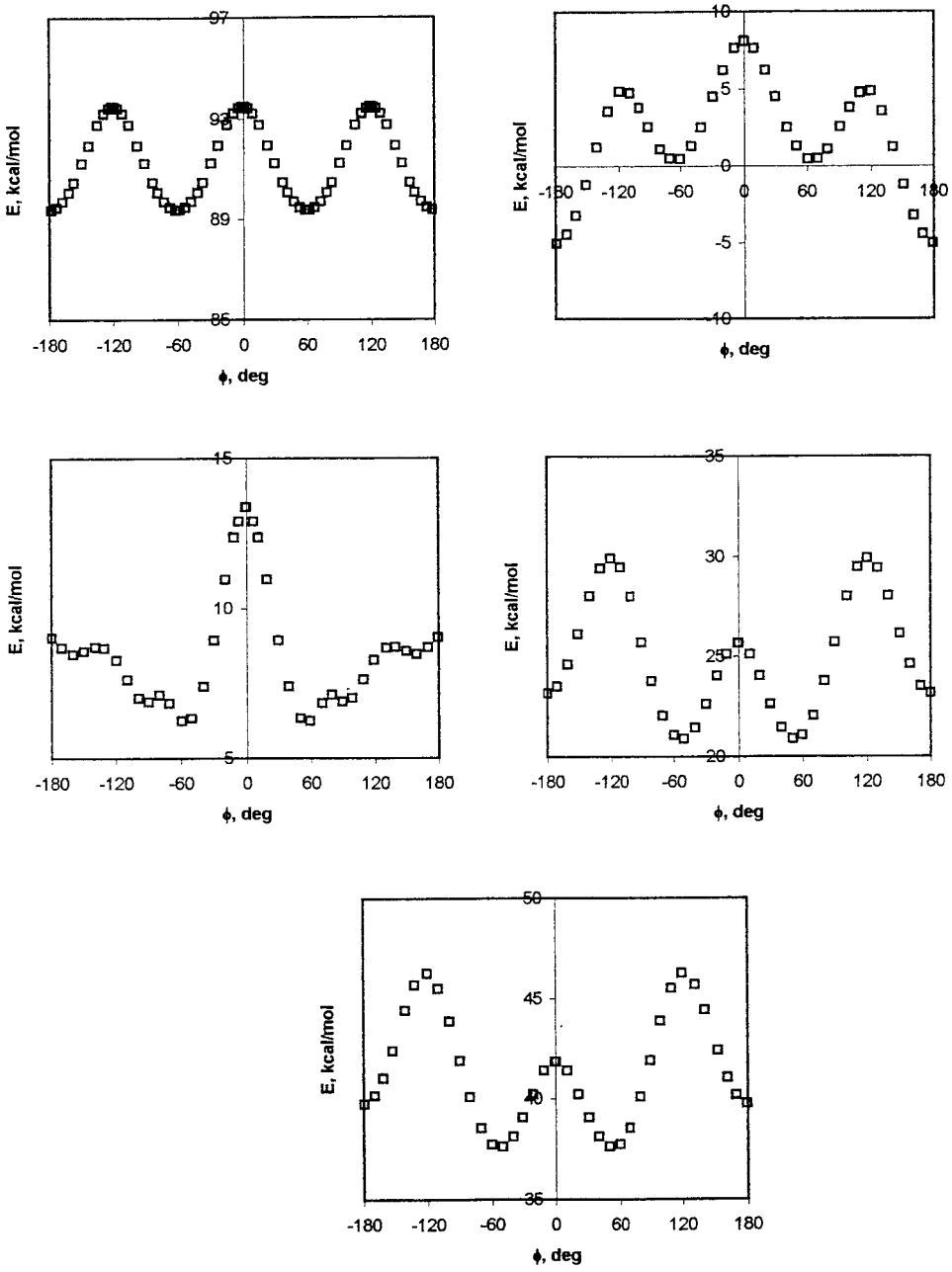

Figure 2. Torsion potentials for the Nafion side chain.

TABLE 2: Simulation Results; Densities and Diffusion Coefficients of Water and K^+ Counterions in Swollen Nafion Membranes at 298 K and 1 atm

system	water content weight %	ρ g/cm^3 simul	ρ g/cm^3 explt	$D_{H2O} \times 10^{11}$ m^2/s simul	$D_{H2O} \times 10^{11}$ m^2/s explt	$D_{K^+} \times 10^{11}$ m^2/s simul
I	5.0	2.01	1.99[a] 1.98[b]	0.22	0.65−0.70[c]	0.17
II	12.5	1.79	1.72[a] 1.93[b]	0.60	1.3−2.3[c]	0.47
III	17.0	1.69		1.3		1.1

[a] Interpolated from reference 8. [b] Interpolated from reference 33. [c] Reference 32.

Naturally, as the water content increases the density decreases. The calculated densities of systems I and II are in a satisfactory agreement with the experimental values (Table 2).

5.2 Radial Distribution Functions. The local structure in hydrated Nafion membranes was characterized in terms of radial distribution functions (RDFs). All RDFs reflect segregation in the solvated membrane. The segregation becomes more pronounced as the water content increases. For example, Figure 3 shows the $O_{H_2O} - O_{H_2O}$ RDFs in systems. In system I, the short-range correlations in water molecule positions are quite prominent, no correlations above 10 Å are observed. At the highest water content (17 wt %, system III), the $O_{H_2O} - O_{H_2O}$ RDF stays above one up to $r \sim 20$ Å, reflecting the tendency for water molecules to congregate. A substantial tendency to congregation is reflected by the S−S RDF at higher water contents (Figure 4). The opposite trends are observed for the $C_{CF_2} - O_{H_2O}$ correlations.

The K−S RDF exhibits a strong peak at ca. 3.6 Å, showing the tendency for counterions to stay in the very vicinity of SO_3^- groups. The peak shifts to larger distances and levels as the water content increases. In system I (5 wt % H_2O), more than 99% of K^+ stay within 4 Å of "their" SO_3^- groups, which means that the counterion migration is practically negligible. However,

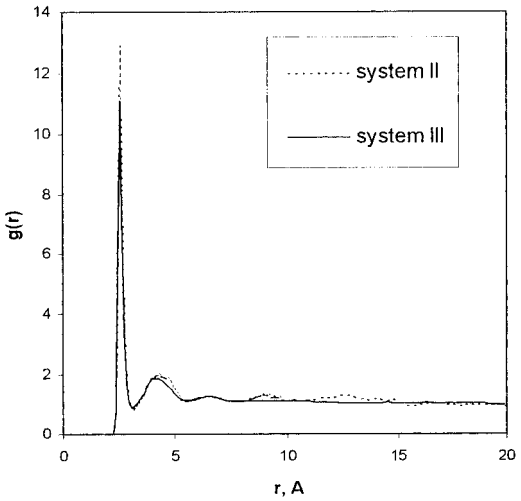

Figure 3. $O_{H_2O}-O_{H_2O}$ radial distribution functions in system III

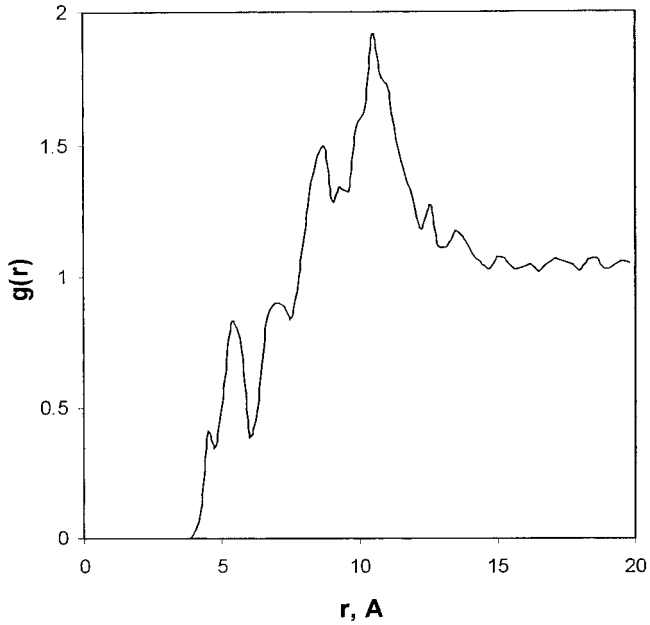

Figure 4. S−S radial distribution functions in system III.

the mobility of the counterion becomes appreciable at a higher water content. The mobilities of water and counterions are discussed below (Section 5.5).

5.3. Morphology of Microsegregation. In hydrated Nafion membranes, one distinguishes a hydrophilic (aqueous) subphase, formed by the solvent (in our case, water) and positively charged counterions around the SO_3^- groups, and a hydrophobic (organic) subphase, formed by the neutral perfluorohydrocarbon skeleton.

To analyze the morphology of the subphases, each point of the simulation cell at a particular time should be assigned to either the aqueous or the organic subphase. We define the hydrophilic subphase as the geometrical locus of points which lie within a certain distance a from any water oxygen atom, SO_3^- oxygen atom, or K^+ counterion. The rest of the space is assigned to the hydrophobic subphase. That is, all water molecules, SO_3^- groups, and counterions belong to the hydrophilic subphase. The value of a determines the hydrophilic subphase connectivity. Let us denote the continuous regions of the hydrophilic subphase as clusters. Then, any two water molecules, counterions, or SO_3^- groups separated by a distance smaller than $l_{bond} = 2a$ belong to the same cluster. We define

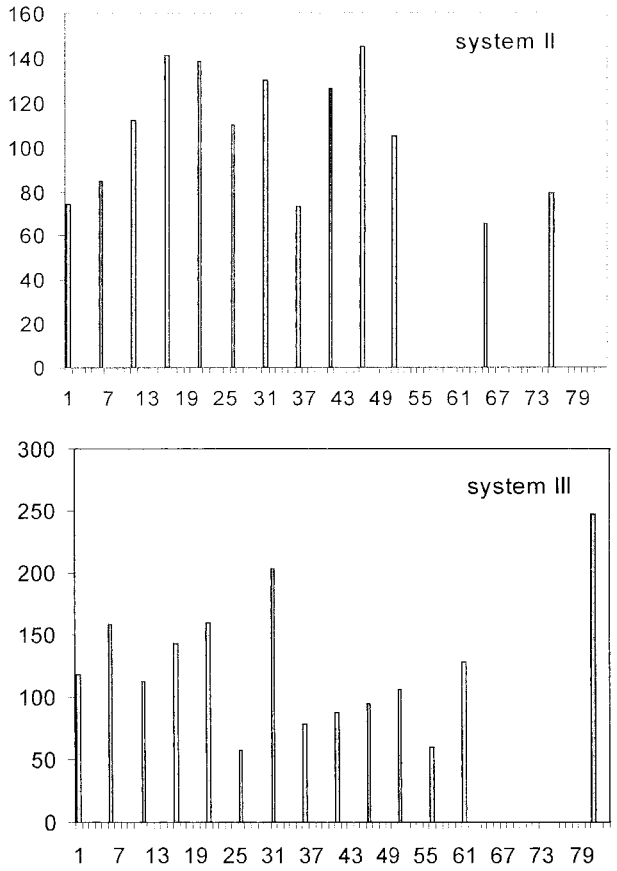

Figure 5. Distributions of a number of water molecules in clusters of different sizes in the final snapshots in systems II (a) and III (b).

the distance to a water molecule as the distance to the center of the oxygen atom, and the distance to an SO_3^- group as the distance to the nearest oxygen of the group. The distance l_{bond} will be referred to as the maximum bond distance, by analogy with the bond distance in percolation theories. The cluster size distributions depend on l_{bond}, with the choice of the latter being somewhat arbitrary. Each cluster is characterized by its volume, shape, and the number of atoms of each component. The hydrophobic subphase was continuous in all three systems.

First, we analyzed the cluster size distribution at $l_{bond} = 0.45$ nm, which approximately corresponds to the second peak of the O−O radial distribution function for bulk SPC/E water. At the lowest water content (system I), most of the water molecules are localized around individual SO_3^- groups in small clusters, which contain 1−5 water molecules and 1 K^+ ion. As the degree of solvation increases, larger hydrophilic clusters are formed. However, even at the 17 wt % water content (system III), the hydrophilic subphase consisted of disconnected clusters, which contained up to 100 water molecules. This is an unexpected result which contradicts the conventional model of a water cluster network.

In Figure 5, we give the distributions of hydrophobic clusters by the number of water molecules in the final configurations of systems II and III. A large portion of small clusters contributing to the very first peak on the histograms do not contained ions and represent isolated water molecules sequested in the hydrophobic subphase. Other small hydrophilic clusters are usually formed around a single SO_3^- group and contain one K^+ ion. Relatively large clusters (more than 50 molecules) in system II are usually surrounded by one SO_3^- group and one K^+ ion per eight water molecules. A snapshot of large clusters in system II is shown in Figure 6.

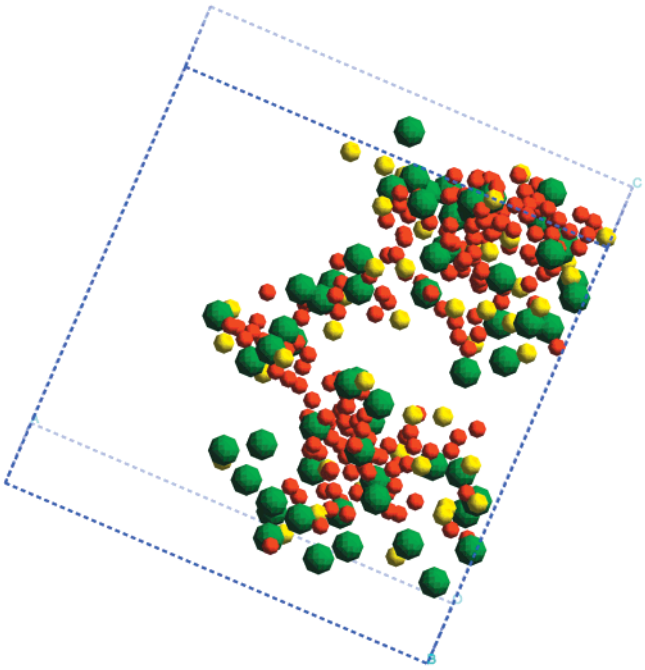

Figure 6. Snapshot of large aqueous cluster with surrounding SO_3^- groups and K^+ ions in system II. Water is shown in red, sulfur in yellow, and potassium in green.

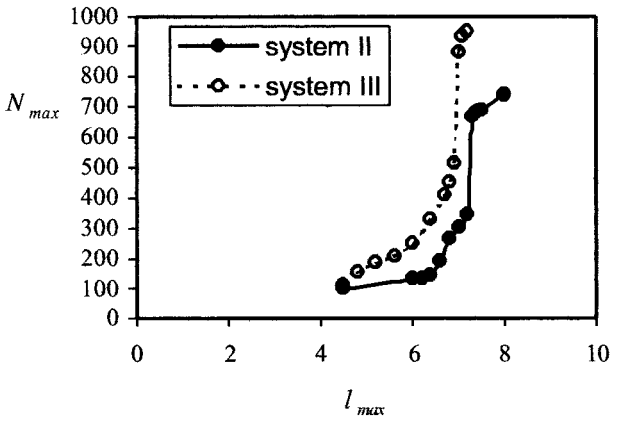

Figure 7. The dependence of the size of the largest cluster in system III on l_{bond}.

It was already mentioned that the sizes of the hydrophilic clusters strongly depend on the maximum bond distance l_{bond}, and there is no clear criterion for the choice of l_{bond}. At sufficiently large l_{bond}, a continuous hydrophilic phase would always be observed. Typically, the dependence of the largest cluster size on l_{bond} would show a percolation-type transition from a set of individual clusters to a single large cluster spanning the simulation box. The dependence of the largest cluster size on the maximum bond distance is shown in Figure 7. In system II, the formation of a single spanning cluster occurs at $l_{bond} \approx 0.73$ nm (see Figure 7). This means that relatively large hydrophilic clusters obtained at $l_{bond} \approx 0.45$ nm are usually separated from each other by one CF_x group, i.e., it is correct to state that there is no continuous hydrophilic subphase in our simulations. The same remains true for system III, where a single cluster is formed at $l_{bond} \approx 0.69$ nm.

Figure 8 shows the evolution of hydrophilic clusters over the trajectory in system II. It should be noted that a significant fraction of molecules is contained in the small clusters comprised of 30 or less water molecules in all three systems. In system I it is close to 100%, while in system III only 30% of water molecules belong to the small clusters. The cluster size distribution in system II shows that the number of molecules in small clusters remains roughly constant throughout the simulation, while the larger clusters (containing more than 50 water molecules) undergo significant modifications. Similar tendencies were found in system III. It is clear that the cluster structure changes considerably from one snapshot to another, with the time interval between the snapshots being ca. 200 ps. Thus, in our simulations, the water molecules are able to "travel", even in the absence of continuous paths of hydrophilic phase, and form temporary bridges between large clusters.

Therefore, the mechanism of water transport in our MD simulations differs from that in the conventional cluster model, which implies that, as the water content increases, the system exhibits a percolation transition from an array of individual clusters to a connected network (i.e., spanning cluster). Instead, we have a dynamic system of clusters, which form and break up on a time scale of roughly 100 ps. These clusters are much smaller than proposed in reference 7; rather, they are close to the pore widths estimated in reference 15. The transport of water and counterions in such a system occurs by coalescence and separation of individual clusters, i.e., instead of "channels" between the clusters, we should consider short-lived bridges. Since the characteristic size of an intermolecular bridge is about $l_{bridge} = 0.3-0.5$ nm, and the bridge formation/breakup time $\tau_{bridge} = 100$ ps, the mobility of bridge-forming water molecules can be evaluated by a diffusion coefficient of $2l_{bridge}/\tau_{bridge} = 10^{-5}$. This corresponds to the self-diffusion coefficient in bulk water.

5.4. Diffusion. Using the Einstein relation, we calculated the translation self-diffusion coefficients of water and K^+ ions. Visual observation and geometric analysis show that in none of the systems does water form a continuous subphase spanning the simulation cell. Note, the Einstein relation always yields a vanishing self-diffusion coefficient for a fluid confined in a cell of finite size, provided that the observation time is unlimited. However, in complex systems like those considered here, the mean square displacement may exhibit intermediate asymptotics within different time intervals. By analogy, if the network of water clusters were not evolving (as in system I), the self-diffusion coefficients of all species should vanish at a sufficiently large (practically unachievable) observation time. However, in real MD simulations the observation time is limited, and the dependence of the mean square displacement on time might show standard features with a linear interval, which allows one to estimate the self-diffusion coefficients even in the systems of limited size.[39] This means that one has to discern between the water motion within the same cluster of the hydrophilic phase and the overall diffusion process, which includes the evolution of the hydrophilic subphase. As the observation time increases, the contribution of the intracluster motion to the diffusion coefficient diminishes. However, if the simulation is not long enough, the water diffusion coefficient obtained with the Einstein relationship reflects the intracluster motion. In the present work, we are unable to distinguish between the intracluster and intercluster motion of water molecules.

The mean square deviations of water molecules in system II are shown in Figure 9. The linear interval begins at ca. 250 ps; the correlation coefficient to the linear regression exceeds 0.995. Similar behaviors were obtained in the other systems. Note that the mean square displacement of a water molecule was about 5 Å within a 1ns time interval. Thus, the estimated diffusion coefficients cannot be attributed to the intercluster transport.

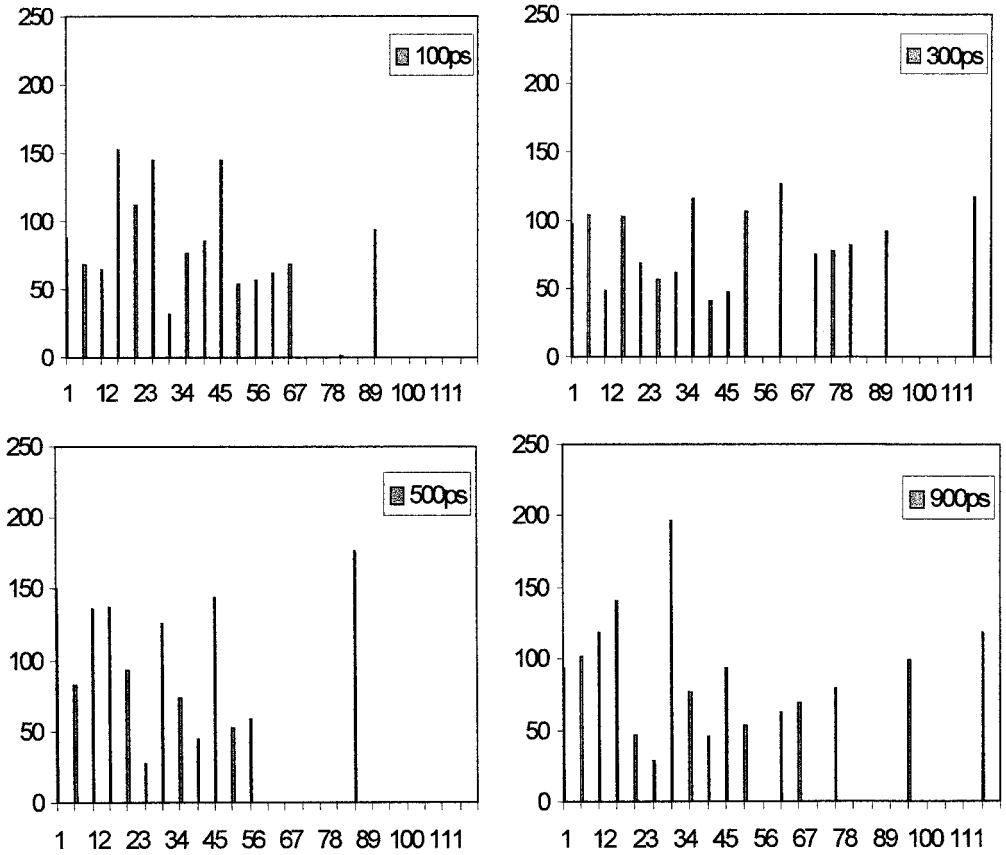

Figure 8. Evolution of the complex of aqueous domains in system II. Diagrams show distribution of number of water molecules in clusters of different sizes in the snapshots of molecular configurations taken at four different moments of the trajectory. Captions show time passed since the beginning of averaging.

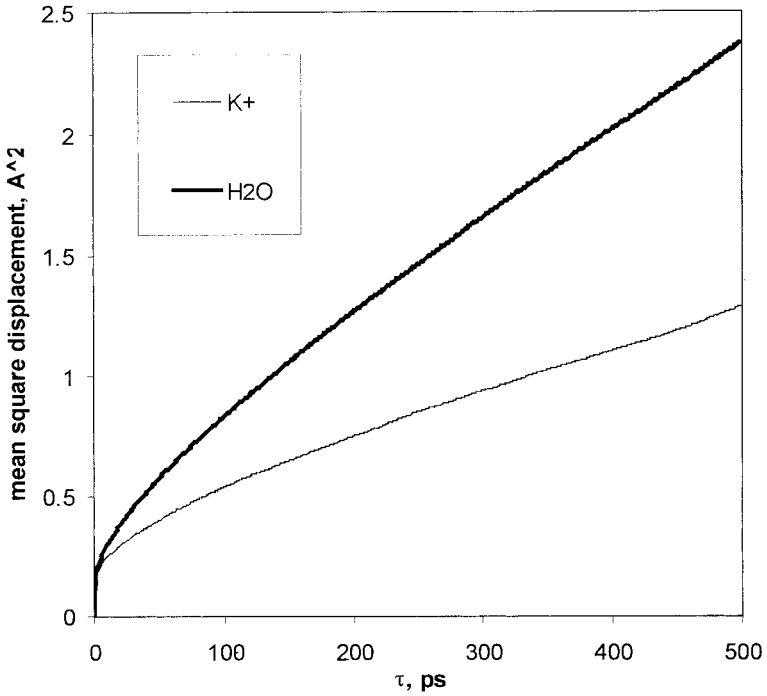

Figure 9. Mean square displacement for water and counterions in system II.

They mostly reflect the intracluster motion of the mobile species. To estimate the intercluster mobilities, simulations of larger fragments of the membrane are required.

It should be noted that different water molecules contribute differently to the overall mean square displacement. Some molecules are surrounded by the perfluorocarbon skeleton or adsorbed on a single SO_3^- group throughout the trajectory (Figure 10, top), while the others belong to the evolving system of water clusters and experience significant displacement during the simulation (Figure 10, middle). The mobility of such molecules may be different over different sections of the trajectory (Figure 10, bottom).

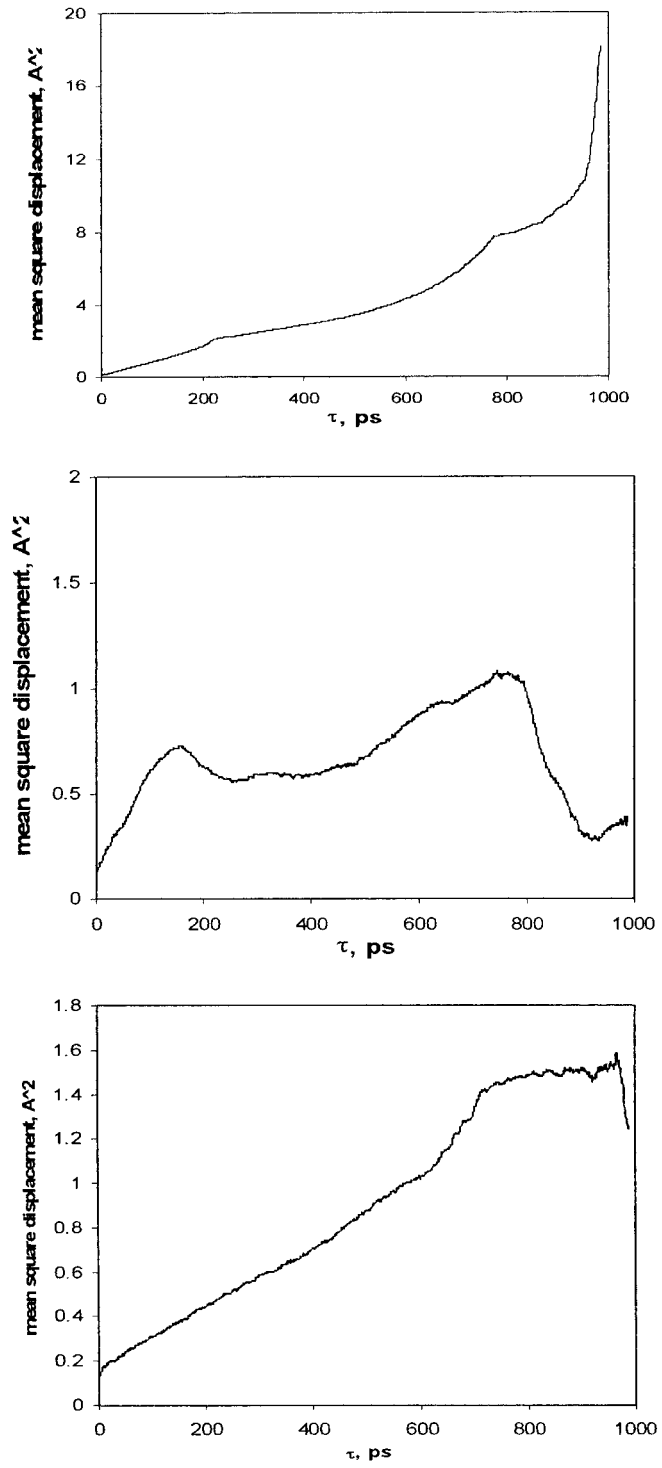

Figure 10. Time dependence of the square displacement of two water molecules in system II; a) mobile water molecule b) immobilized water molecule surrounded by perfluorocarbon skeleton.

The calculated self-diffusion coefficients of water and the counterions are presented in Table 2. The diffusion coefficients for SO_3^- groups are given for comparison. They reflect the overall fluctuations of the polymer chains. In system I, water is practically immobilized. The water diffusion coefficient is of the same order of magnitude as the diffusion coefficients for SO_3^- groups, and the counterion diffusion coefficient is almost equal to that of SO_3^- group. The experimental diffusion coefficient of water is about twice as high.

In system II, the diffusion coefficients of water and counterions are several times higher than that of SO_3^- groups. We conclude that the diffusion coefficients of the mobile species reflect the evolution of the system of hydrophilic clusters rather than just thermal fluctuations in the system. Table 2 also shows that the water diffusion coefficient increases visibly from system II to system III, while the diffusion coefficients of SO_3^- group are practically the same in the two systems. The experimental diffusion coefficient of water measured by the U.S. Army NSC [32] is substantially higher than the MD estimate. However, there are several factors which are to be considered in order to compare the simulation results with the experiment. First, the samples of Nafion with K^+ as the counterion were obtained by boiling the corresponding acid form samples in KOH.[32] The protons were not completely replaced by the potassium counterions. The molar fraction of K^+ counterions is approximately 70% in samples I and II. Second, the experimental diffusion coefficients were calculated from the water transport through a Nafion film, i.e., these quantities differ from the average self-diffusion coefficients obtained from the Einstein relationship.

6. Conclusion

We developed a molecular forcefield for Nafion membranes with a united atom presentation of the perfluorocarbon skeleton. Using this forcefield, we performed a series of 1 ns simulations of hydrated Nafion membranes (with K^+ as the counterion) at varying water content. Microphase segregation in the hydrated membranes was observed. Reasonable agreement with experimental densities and water diffusion coefficients was obtained. It was found that that water does not form a continuous subphase. Rather, at higher water content close to the experimental saturation conditions, we observed isolated clusters of about 100 water molecules. The system of hydrophilic clusters evolves in time; short living bridges are formed between the clusters, causing their coalescence and break up.

Based on the above observations, we propose the following qualitative picture of water transport in the membranes. Since the mobility of SO_3^- groups is much smaller than those of water and the counterions, we may consider SO_3^- as immobilized. They are surrounded by hydrophilic clusters, which may contain up to 100 water molecules. The hydrophilic clusters are effectively connected by short lived bridges. The frequency of intercluster bridge formation is as large as $(100\text{ps})^{-1}$. That means that the effective mobility of water molecules that form intercluster bridges is of the same order as the mobility of molecules in the bulk water ($10^{-5}\text{cm}^2/\text{s}$). The overall water diffusion coefficients obtained from the mean square displacement data are on the order of $10^{-7}\text{cm}^2/\text{s}$ and mostly reflect the transport within the clusters. We conclude that the mechanism of water transport in our MD simulations differs from that in the conventional cluster model, which assumes a continuous hydrophilic subphase. Instead, we put forward a model of a dynamic system of clusters with temporary intercluster bridges. Due to a broad deviation in mobilities of differently located water molecules and the insufficient length of the simulation, it is problematic to distinguish between the inter- and intracluster motion in the simulation. However, the fact that the diffusion coefficients obtained are on the same order of magnitude as the experimental transport coefficients through the membrane allows us to suppose that the intercluster motion is unlikely a limiting stage of the water and counterion transport.

It is clear that the size of the simulation box in the present work was not sufficient to make a clear conclusion about the real processes in hydrated Nafion membranes. However, based on the simulation result, we assume that it is not necessary for the hydrophilic phase to be continuous in order to yield a

diffusion coefficient as high as experimentally observed. Computer experiments with larger systems, including mesoscale simulations, may shed light of the morphology of segregation and transport in ion-exchange membranes of the Nafion type.

Acknowledgment. Research is supported by the U.S. Army NSC. The authors thank Dr. Rivin for stimulating discussions.

References and Notes

(1) Gray, F. M. *Solid Polymer Electrolites: Fundamental and Technological Applications*; VCH Publishers Inc.: New York, 1991.
(2) *Polymer Modified Electrodes: Preparation and Characterisation, in: Electrochemical Science and Technology of Polymers − 1*; Hillman, A. R., Ed.; Elsevier Applied Science: London, New York, 1990; p 102.
(3) Penner, S. S.; Appleby, A. J.; Baker, B. S.; Bates, J. L.; Buss, L. B.; Dollard, W. J.; Farns, P. J.; Gillis, E. A.; Gunsher, J. A.; Khandkar, A.; Krumpelt, M.; Osullivan, J. B.; Runte, G.; Savinell, R. F.; Selman, J. R.; Shores, D. A.; Tarman, P. *Energy* **1995**, *20*, 331.
(4) Timonov, A. M. *Soros Educ. J.: Chem.* **2000**, *6*, 69.
(5) Sakai, T.; Takenaka, H.; Torikai, E. *J. Electrochem. Soc.* **1986**, *133*, 88.
(6) *Ionomers*; Tant, M. R., Maurotz, K. A., Wilkes, G. L., Ed.; Blackie Academic & Professional: London, 1997.
(7) Gierke, T. D.; Hsu, W. Y. *ACS Symposium Series* **1982**, *180*, 283.
(8) Gierke, T. D.; Munn, G. E.; Wilson, F. C. *J. Polym. Sci., Part B: Polym. Phys.* **1981**, *19*, 1687.
(9) Mauritz, K. A.; Rogers, C. E. *Macromolecules* **1985**, *18*, 483.
(10) Eikerling, M.; Kornyshev, A. A.; Stimming, U. *J. Phys. Chem. B* **1997**, *101*, 10807.
(11) Pineri, M.; Duplessix, R.; Volino, F. *ACS Symposium Series* **1982**, *180*, 249.
(12) Falk, M. *Can. J. Chem.* **1980**, *58*, 1495.
(13) Plate, N. A.; P., S. V. *Brush-Like Polymers and Liquid Crystalls*; Khimija: Moscow, 1980.
(14) Timashev, S. F. *Physical chemistry of membrane processes*; Khimija: Moscow, 1988.
(15) Tovbin, Y. K. *Zh. Fiz. Khim.* **1998**, *72*, 55.
(16) Ozerin, A. N.; Rebrov, A. V.; Yakunin, A. N.; Bessonova, N. P.; Dreiman, N. A.; Sokolov, N. F.; Bakeev, L. F. *Vysokomol. Soedin. Ser. A* **1986**, *28*, 2303.
(17) Meresi, G.; Wang, Y.; Bandis, A.; Inglefield, P. T.; Jones, A. A.; Wen, W. Y. *Polymer* **2001**, *42*, 6153.
(18) Elliott, J. A.; Hanna, S.; Elliott, A. M. S.; Cooley, G. E. *Macromolecules* **2000**, *33*, 4161.
(19) James, P. J.; Elliott, J. A.; McMaster, T. J.; Newton, J. M.; Elliott, A. M. S.; Hanna, S.; Miles, M. J. *J. Mater. Sci.* **2000**, *35*, 5111.
(20) Gebel, G. *Polymer* **2000**, *41*, 5829.
(21) Orfino, F. P.; Holdcroft, S. *J. New Mater. Electrochem. Syst.* **2000**, *3*, 285.
(22) Gong, X.; Bandis, A.; Tao, A.; Meresi, G.; Wang, Y.; Inglefield, P. T.; Jones, A. A.; Wen, W. Y. *Polymer* **2001**, *42*, 6485.
(23) Paddison, S. J.; Zawodzinski, T. A. *Solid State Ion.* **1998**, *115*, 333.
(24) Vasyutkin, N. F.; Tovbin, Y. K. *Vysokomol. Soedin.* **1993**, *35*, A1600.
(25) Din, X. D.; Michaelides, E. E. *AICHE J.* **1998**, *44*, 35.
(26) Dyakov, Y. A.; Tovbin, Y. K. *Russ. Chem. Bull.* **1995**, *44*, 1186.
(27) Ennari, J.; Elomaa, M.; Sundholm, F. *Polymer* **1999**, *40*, 5035.
(28) Lyubartsev, A. P.; Laaksonen, A. *J. Biomol. Struct. Dyn.* **1998**, *16*, 579.
(29) Muller-Plathe, F.; van Gunsteren, W. F. *J. Chem. Phys.* **1995**, *103*, 4745.
(30) Vishnyakov, A.; Neimark, A. V. *J. Phys. Chem. B* **2000**, *104*, 4471.
(31) Vishnyakov, A.; Neimark, A. V. *J. Phys. Chem. B* **2000**, in press.
(32) Rivin, D., private communication.
(33) Nandan, D.; Mohan, H.; Iyer, R. M. *J. Membr. Sci.* **1992**, *71*, 69.
(34) Cui, S. T.; Siepmann, J. I.; Cochran, H. D.; Cummings, P. T. *Fluid Phase Equilib.* **1998**, *146*, 51.
(35) Dixon, D. A.; van Catledge, F. A. *Int. J. Supercomput. Appl. High Perform. Comput.* **1988**, *2*, 62.
(36) Berendsen, H. J. C.; Grigera, J. R.; Straatsma, T. P. *J. Phys. Chem.* **1987**, *91*, 6269.
(37) Heinzinger, K. *Physica B & C* **1985**, *131*, 196.
(38) Verlet, L. *Phys. Rev.* **1967**, *159*, 98.
(39) Vishnyakov, A.; Piotrivskaya, E. M.; Brodskaya, E. N. *Zh. Fiz. Khim.* **1999**, *73*, 519.